Supporting Information

A Tumor-targetable NIR Probe with Photoaffinity Crosslinking Characteristics for Enhanced Imaging-Guided Cancer Phototherapy

Rui Sun,‡ Yuqi Zhang,‡ Yinjia Gao, Meng Zhao, Anna Wang, Jinfeng Zhu, Xiaju Cheng,* Haibin Shi,*

State Key Laboratory of Radiation Medicine and Protection, School for Radiological and Interdisciplinary Sciences (RAD-X) and Collaborative Innovation Center of Radiation Medicine of Jiangsu Higher Education Institutions, Soochow University, Suzhou 215123, P. R. China

* Co-corresponding author: xjcheng@suda.edu.cn; hbshi@suda.edu.cn

‡ Run Sun and Yuqi zhang contributed equally to this work

Table of Contents

Chemical synthesis and characterization of probes

Synthesis of (9H-fluoren-9-yl) methyl-tert-butyl(6-oxo-6-(prop-2-yn-1-ylamino) hexane-1,5-diyl) (S)-dicarbamate (1). To a solution of propargylamine (0.29 mL) in DMF (30 mL), coupling reagent HOBt (0.68 g, 5.04 mmol), HBTU (1.91 g, 5.04 mmol) and DIPEA (1.08 g, 8.4 mmol) were added. Fmoc-Lys (Boc)-COOH (1.97 g, 4.2 mmol) was then added to the above solution and the reaction was stirred at r.t. overnight. Subsequently, the reaction was quenched with ddH_2O and EA. The organic layer was washed with ddH_2O (30 mL), sodium bicarbonate solution (30 mL), brine (30 mL). The organic layer was concentrated and purified by column chromatography to afford compound **1** as white solid in 92% yield. ^{1}H NMR (400 MHz, DMSO-d6), δ (ppm): 8.35 (s, 1H), 7.90 (d, *J* = 7.5 Hz, 2H), 7.74 (dd, *J* = 7.2, 4.3 Hz, 2H), 7.48 (d, *J* = 8.2 Hz, 1H), 7.42 (t, *J* = 7.4 Hz, 2H), 7.34 (t, *J* = 7.4 Hz, 2H), 6.77 (t, *J* = 5.1 Hz, 1H), 4.25 (m, 3H), 3.95 (d, *J* = 5.1 Hz, 1H), 3.86 (dd, *J* = 5.2, 2.3 Hz, 2H), 3.10 (t, *J* = 2.5 Hz, 1H), 2.89 (d, *J* = 2.7 Hz, 2H), 1.56 (dd, *J* = 10.2, 4.1 Hz, 2H), 1.37 (s, 11H), 1.23 (s, 2H); ^{13}C NMR (101 MHz, $CDCl_3$), δ (ppm): 171.02, 155.84, 143.24, 140.82, 127.29, 126.63, 124.59, 119.53, 78.77, 71.29, 66.61, 54.15, 46.65, 31.49, 29.16, 28.71, 27.96, 21.94.

Synthesis of (9H-fluoren-9-yl) methyl (S)-(6-amino-1-oxo-1-(prop-2-yn-1-ylamino) hexan-2-yl) carbamate (2). A mixed solution containing trifluoroacetic acid and dichloromethane (1:4) (20 mL) was added to compound **1** (1.01 g, 2 mmol) and stirred for 1 h at r.t. The reaction mixture was evaporated under vacuo, and the resultant residue was diluted with 1 M NaOH (30 mL), extracted with dichloromethane for three times (30 mL/time). The organic phase was dried with anhydrous $MgSO_4$ and then concentrated in vacuo to obtain crude product which appeared as white solid after purification with silica gel flash chromatography (0.65 g, 80%). ^{1}H NMR (400 MHz, DMSO-d6), δ (ppm): 8.43 (s, 1H), 7.93 (d, *J* = 7.5 Hz, 2H), 7.82 (s, 2H), 7.77 (t, *J* = 7.2 Hz, 2H), 7.55 (d, *J* = 8.3 Hz, 1H), 7.46 (t, *J* = 7.3 Hz, 2H), 7.37 (t, *J* = 7.4 Hz, 2H), 4.31 (d, *J* = 6.5 Hz, 2H), 4.26 (d, *J* = 6.2 Hz, 1H), 3.99 (dd, *J* = 13.6, 8.9 Hz, 1H), 3.90 (dd, *J* = 5.3, 2.3 Hz, 2H), 3.15 (t, *J* = 2.4 Hz, 1H), 2.80 (d, *J* = 5.4 Hz, 2H), 1.61 (m, 4H), 1.36 (m, 2H); ^{13}C NMR (101 MHz, DMSO-d6), δ (ppm): 171.69, 155.98, 143.81, 140.70, 127.62, 127.05, 125.29, 120.10, 81.03, 73.02, 65.59, 54.22, 46.64, 31.17, 27.94, 26.52, 22.40.

Synthesis of (9H-fluoren-9-yl)methyl(S)-(6-(3-(3-methyl-3H-diazirin-3-yl)propanamido)-1-oxo-1-(prop-2-yn-1-ylamino)hexan-2-yl)carbamate (3). Into 15 mL anhydrous DCM solution containing NHS-diazirine (0.25 g, 1 mmol), compound **2** (0.41 g, 1 mmol) and Et_3N (278 μL, 2 mmol) were introduced and the reaction mixture was stirred at room temperature for 2 h. The reaction mixture was then washed with ddH_2O for three times (25 mL/time) and brine for one time (25 mL). The organic layer was concentrated and purified by column chromatography to afford compound **3** as white solid in 95% yield. ^{1}H NMR (400 MHz, DMSO-d6), δ (ppm): 8.30 (s, 1H), 7.86 (d, *J* = 7.5 Hz, 2H), 7.78 (s, 1H), 7.70 (t, *J* = 7.0 Hz, 2H), 7.43 (d, *J* = 8.2 Hz, 1H), 7.39 (t, *J* = 7.4 Hz, 2H), 7.30 (t, *J* = 7.4 Hz, 2H), 4.21 (dt, *J* = 16.2, 6.8 Hz, 3H), 3.90 (dd, *J* = 13.7, 8.8 Hz, 1H), 3.82 (d, *J* = 2.9 Hz, 2H), 3.07 (s, 1H), 2.97 (dt, *J* = 14.0, 7.0 Hz, 2H), 1.90 (t, *J* = 7.7 Hz, 2H), 1.52 (m, 4H), 1.34 (dd, *J* = 14.1, 7.2 Hz, 2H), 1.24 (d, *J* = 39.2 Hz, 2H), 0.93 (s, 3H); ^{13}C NMR (101 MHz, DMSO-d6), δ (ppm): 172.22, 170.88, 156.37, 144.26, 141.13, 128.06, 127.48, 125.76, 120.52, 81.49, 73.43, 66.05, 54.83, 47.09, 31.95, 30.24, 29.13, 28.36, 19.74.

Synthesis of (S)-2-amino-6-(3-(3-methyl-3H-diazirin-3-yl)propanamido)-N-(prop-2-yn-1-yl)

hexanamide (4). A mixed solution containing piperidine and N, N-dimethylformamide (1:4) (10 mL) was added to compound **3** (0.5 g, 0.97 mmol) and stirred for 1 h at r.t. The reaction mixture was concentrated and purified with silica gel flash chromatography to afford compound **4** as pale yellow oil (0.2 g, 70%). ^{1}H NMR (400 MHz, DMSO-d6), δ (ppm): 8.25 (s, 1H), 7.84 (s, 1H), 3.88 (s, 2H), 3.42 (s, 2H), 3.14 (d, *J* = 7.1 Hz, 1H), 3.11 (m, 1H), 3.03 (dd, *J* = 12.5, 6.6 Hz, 2H), 1.97 (t, *J* = 7.7 Hz, 2H), 1.60 (d, *J* = 8.0 Hz, 2H), 1.38 (m, 4H), 1.27 (d, *J* = 5.8 Hz, 2H), 1.01 (s, 3H); ^{13}C NMR (101 MHz, DMSO-d6), δ (ppm): 174.99, 170.43, 81.29, 72.75, 54.47, 34.71, 29.78, 28.95, 27.73, 25.80, 22.65, 19.29.

Synthesis of 3-(2-carboxyethyl)-2-((1E, 3E, 5E, 7E)-7-(1,1-dimethyl-3-(3-(((S)-6- (3-(3-methyl-3H-diazirin-3-yl)propanamido)-1-oxo-1-(prop-2-yn-1-ylamino)hexan-2-yl) amino)-3-oxopropyl)-1,3-dihydro-2H-benzo[e]indol-2-ylidene)hepta-1,3,5-trien-1-yl)-1,1-dimethyl-1H-benzo[e]indol-3-ium (5). A DMF solution (5 mL) containing HOBt (4.7 mg, 0.035 mmol), EDC (6,7 mg, 0.035 mmol), and cypate (18.1 mg, 0.029 mmol) was stirred at room temperature for 20 min. Compound **4** (10.3 mg, 0.035 mmol) was then added to the reaction mixture. After 8 h the reaction mixture was separated by HPLC using MeCN and H_2O containing 0.1% of TFA as eluents to afford compound **5** as cyanic solid powder (15.1 mg, 58%). ^{1}H NMR (400 MHz, $CDCl_3$), δ (ppm): 11.36 (s, 1H), 9.62 (s, 1H), 8.99 (s, 1H), 8.12 (dd, *J* = 8.3, 4.5 Hz, 2H), 7.98 (dd, *J* = 19.3, 8.4 Hz, 4H), 7.82 (s, 1H), 7.65 (dt, *J* = 15.5, 8.0 Hz, 3H), 7.51 (m, 2H), 7.42 (d, *J* = 9.4 Hz, 1H), 6.59 (s, 1H), 6.31 (s, 1H), 5.46 (s, 5H), 4.59 (dd, *J* = 7.5, 5.7 Hz, 1H), 4.44 (m, 2H), 4.00 (d, *J* = 3.6 Hz, 2H), 3.39 (d, *J* = 5.4 Hz, 2H), 3.22 (s, 3H), 2.06 (dd, *J* = 11.4, 5.9 Hz, 6H), 1.99 (d, *J* = 3.3 Hz, 6H), 1.71 (m, 2H), 1.46 (d, *J* = 9.2 Hz, 6H), 1.33 (d, *J* = 6.6 Hz, 4H), 1.02 (s, 2H), 0.92 (s, 3H); MS (ES+): *m/z* calcd for Chemical Formula: $C_{55}H_{62}N_7O_5^+$ $[M]^+$: 900.4807; Found: 899.9542.

Synthesis of 2-((1E, 3E, 5E, 7E)-7-(3-(3-(((2S)-1-(((1-(3-(4-(4-(((2-amino-4-hydroxyl pteridin-6-yl)methyl)amino)benzamido)-4-carboxybutanamido)propyl)-1H-1,2,3-triazol-4-yl)methyl)amino)-6-(3-(3-methyl-3H-diazirin-3-yl)propanamido)-1-oxohexan-2-yl)amino)-3-oxopropyl)-1,1-dimethyl-1,3-dihydro-2H-benzo[e]indol-2-ylidene)hepta-1,3,5-trien-1-yl)-3-(2-carboxyethyl)-1,1-dimethyl-1H-benzo[e]indol-3-ium (DACF). The cycloaddition reaction was carried out by using compound **6** (9 mg, 0.01 mmol), FA-N_3 (5.2 mg, 0.01 mmol), $CuSO_4$ (0.09 mg, 5 mmol%) as catalyst, sodium ascorbate (0.2 mg, 10 mmol%) as additive in a mixture of DMSO/H_2O (1:1, 1 mL).[1] The reaction was stirred at room temperature for 8 h. After 8 h the reaction mixture was separated by HPLC using MeCN and H_2O containing 0.1% of TFA as eluents to afford compound **DACF** as cyanic solid powder (12.8 mg, 94%). ^{1}H NMR (300 MHz, DMSO-d6) δ 9.24 (s, 1H), 8.82 (d, *J* = 8.5 Hz, 2H), 8.63 (dd, *J* = 8.4, 4.6 Hz, 7H), 8.46 (d, *J* = 7.5 Hz, 2H), 8.32 (d, *J* = 9.0 Hz, 2H), 8.25 (d, *J* = 8.8 Hz, 5H), 8.15 (s, 1H), 8.06 (d, *J* = 7.4 Hz, 2H), 8.03 – 7.79 (m, 7H), 7.56 (t, *J* = 5.4 Hz, 1H), 7.27-7.12 (m, 4H), 7.04 (d, *J* = 13.7 Hz, 2H), 5.14-4.97 (m, 7H), 4.83 (ddd, *J* = 21.1, 11.9, 5.9 Hz, 7H), 3.82 (dd, *J* = 14.7, 3.8 Hz, 1H), 3.62 (dd, *J* = 14.5, 9.8 Hz, 1H), 3.32 (t, *J* = 6.8 Hz, 9H), 2.90 (t, *J* = 7.3 Hz, 4H), 2.62 (d, *J* = 5.8 Hz, 1H), 2.15 (s, 15H), 1.98-1.78 (m, 5H), 1.43 (d, *J* = 6.9 Hz, 1H). ^{13}C NMR (151 MHz, DMSO-d6) δ 174.81, 174.68, 172.87, 172.82, 166.72, 161.72, 156.66, 156.57, 156.07, 154.90, 151.24, 150.51, 149.01, 149.00, 148.99, 148.81, 148.81, 145.11, 144.32, 144.26, 141.17, 140.08, 137.67, 135.60, 133.47, 132.58, 131.66, 130.64, 130.60, 130.56, 130.33, 129.41, 128.39, 128.19, 128.10, 128.00, 127.54, 126.30, 126.25, 125.75, 125.20, 125.12, 122.62, 121.91, 120.57, 112.14, 112.11, 112.08, 111.70, 111.63, 104.21, 104.18, 77.83, 66.03, 54.60, 54.56, 52.71, 50.83, 49.33, 47.15, 46.42, 46.38, 37.23, 35.46, 34.16, 34.16, 33.30, 33.15, 33.12, 33.03, 31.25, 31.18, 31.02, 29.89, 29.60, 28.73,

27.18, 27.00, 23.41, 23.34, 23.10. MS (ES+): *m/z* calcd for Chemical Formula: $C_{77}H_{87}N_{18}O_{10}^+$ $[M]^+$: 1423.6847; Found: 1423.1622.

Synthesis of 2-((1E,3E,5E,7E)-7-(3-(3-(((R)-1-(((1-(3-((R)-4-(4-(((2-amino-4-hydroxypteridin-6-yl)methyl)amino)benzamido)-4-carboxybutanamido)propyl)-1H-1,2,3-triazol-4-yl)methyl)amino)-6-((tert-butoxycarbonyl)amino)-1-oxohexan-2-yl)amino)-3-oxopropyl)-1,1-dimethyl-1,3-dihydro-2H-benzo[e]indol-2-ylidene)hepta-1,3,5-trien-1-yl)-3-(2-carboxyethyl)-1,1-dimethyl-1H-benzo[e]indol-3-ium (CF). A mixed solution containing piperidine (20%) and N, N-dimethylformamide (1:4) (10 mL) was added to compound **1** (0.5 g, 0.97 mmol) and stirred for 1 h at r.t. The reaction mixture was concentrated and purified with silica gel flash chromatography to afford compound **1'** as pale yellow oil (0.18 g, 65%). 5 mL of DMF solution containing HOBt (4.7 mg, 0.035 mmol), EDC (6,7 mg, 0.035 mmol), and cypate (18.1 mg, 0.029 mmol) was stirred at r.t. for 20 min. Compound **1'** (9.9 mg, 0.035 mmol) was then added to the reaction mixture. After 8 h the reaction mixture was separated by HPLC using MeCN and H_2O containing 0.1% of TFA as eluents to afford compound **2'** as cyanic solid powder (19.4 mg, 75%). The cycloaddition reaction was carried out by using compound **2'** (8.91 mg, 0.01 mmol), FA-N_3 (5.2 mg, 0.01 mmol), $CuSO_4$ (0.09 mg, 5 mmol%) as catalyst, sodium ascorbate (0.2 mg, 10 mmol%) as additive in a mixture of DMSO/H_2O (1:1, 1 mL). The reaction was stirred at r.t. for 8 h, and then separated by HPLC using MeCN and H_2O containing 0.1% of TFA as eluents to afford compound **CF** as cyanic solid powder (12.85 mg, 91%). ^{1}H NMR (600 MHz, DMSO-d6) δ 12.51 (s, 3H), 8.63 (s, 2H), 8.36 (d, *J* = 5.4 Hz, 1H), 8.28-8.13 (m, 4H), 8.06-7.89 (m, 6H), 7.88-7.73 (m, 3H), 7.69 (d, *J* = 8.9 Hz, 1H), 7.67-7.43 (m, 7H), 6.67-6.49 (m, 5H), 6.43-6.23 (m, 3H), 5.30 (s, 1H), 4.42 (d, *J* = 47.7 Hz, 6H), 4.24 (d, *J* = 50.7 Hz, 5H), 4.11 (s, 2H), 3.02 (s, 3H), 2.77-2.58 (m, 6H), 2.24 (s, 1H), 2.17 (s, 1H), 1.99 (s, 2H), 1.89 (s, 7H), 1.42 (s, 2H), 1.32 (s, 7H), 1.21 (s, 5H), 1.13 (d, *J* = 22.7 Hz, 4H), 0.83 (s, 2H). ^{13}C NMR (151 MHz, DMSO-d6) δ 174.51, 174.27-174.21, 172.37, 172.08, 171.73, 169.64, 166.72, 163.83, 161.04, 155.91, 151.16, 148.90, 144.95, 140.05, 139.55, 138.66, 133.64, 133.18, 131.75, 131.56, 130.28, 129.53, 129.41, 128.02, 126.22, 125.02, 123.28, 122.57, 121.76, 112.18, 112.01, 111.61, 102.48, 86.74, 79.69, 77.76, 65.10, 64.97, 53.02, 51.00, 50.67, 47.56, 46.34, 41.19, 40.86, 36.18, 35.56, 34.62, 33.82, 32.15, 31.72, 30.44, 29.77, 29.60, 29.46, 29.13, 29.01, 28.69, 27.21, 27.15, 27.08, 25.54, 22.93, 22.54, 14.40. MS (ES+): *m/z* calcd for Chemical Formula: $C_{77}H_{89}N_{16}O_{11}^+$ $[M]^+$: 1413.6891; Found: 1414.7091.

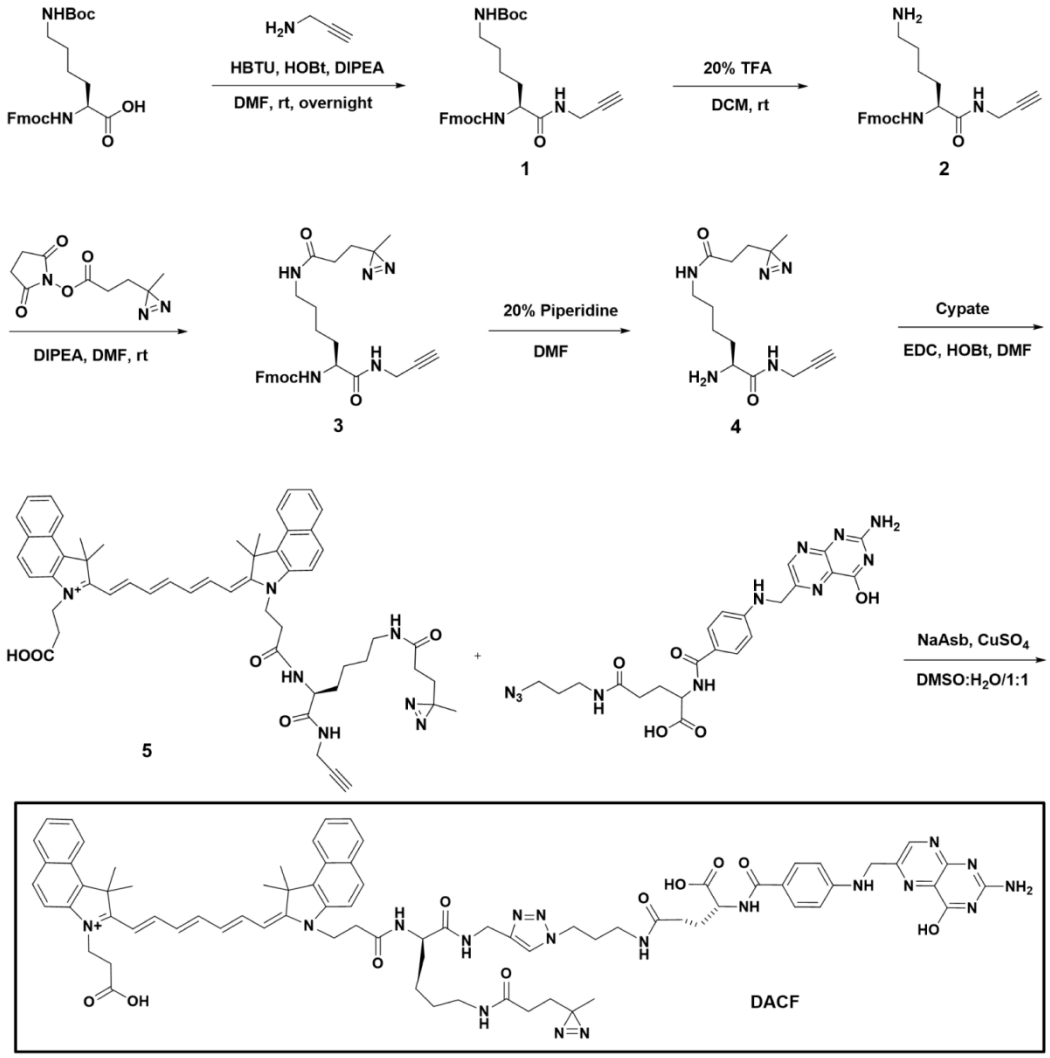

Scheme S1. Synthetic route of probe DACF. HBTU = O-benzotriazole-N,N,N,N’-tetramethyl-uronium-hexafluorophosphate, HOBt = 1-hydroxybenzotriazole, DIPEA = N,N-diisopropylethylamine, DMF = N,N-dimethylformamide, TFA = trifluoroacetic acid, DCM = dichloromethane, EDC = 1-ethyl-3-(3-dimethylaminopropyl)carbodiimide, NaAsb = sodium ascorbate, DMSO = dimethylsulfoxide.

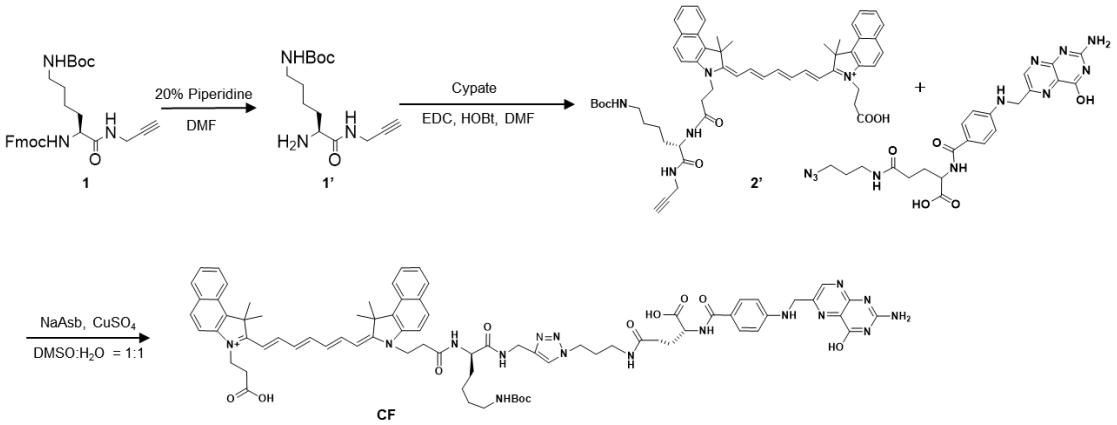

Scheme S2. Synthesis of control probe CF. HOBt = 1-hydroxybenzotriazole, DMF = N,N-dimethylformamide, EDC = 1-ethyl-3-(3-dimethylaminopropyl) carbodiimide, NaAsb = sodium ascorbate, DMSO = dimethylsulfoxide.

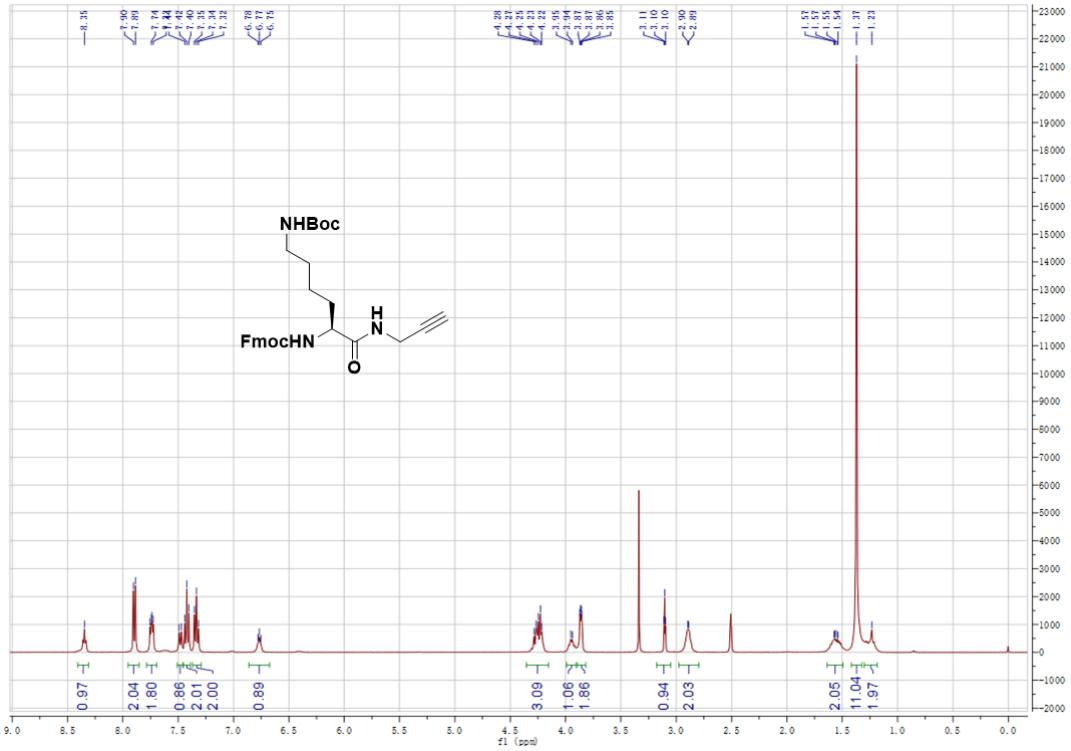

Figure S1. ^{1}H NMR spectrum of compound **1**.

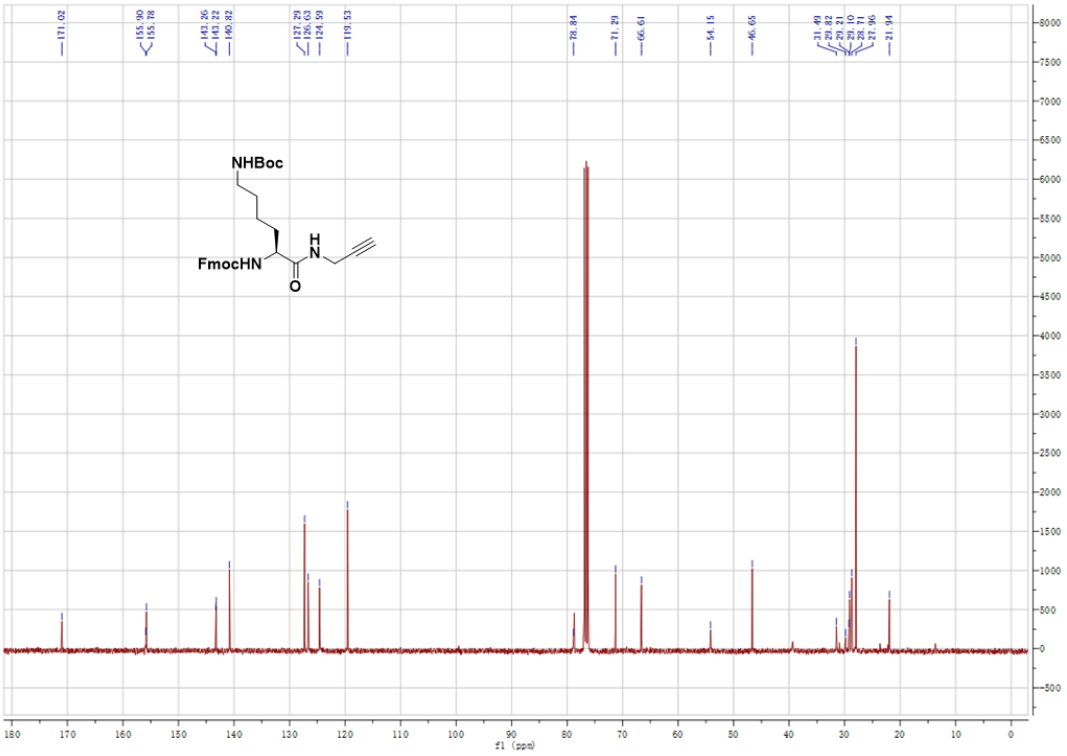

Figure S2. ^{13}C NMR spectrum of compound **1**.

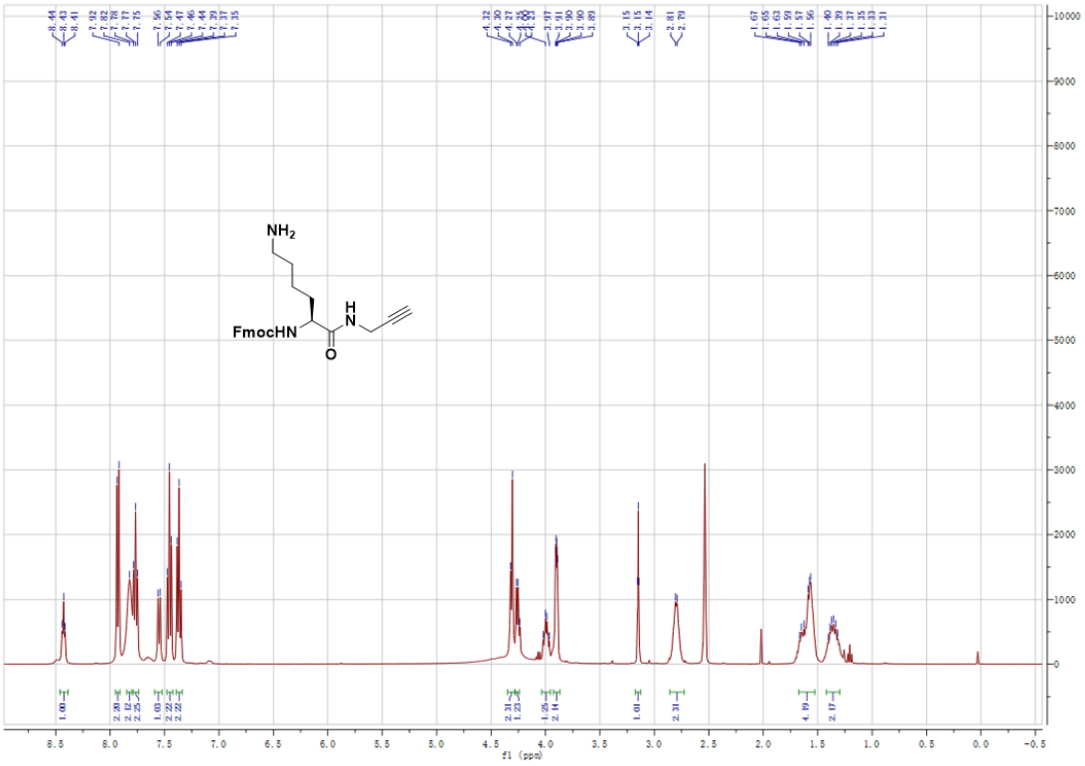

Figure S3. ^{1}H NMR spectrum of compound **2**.

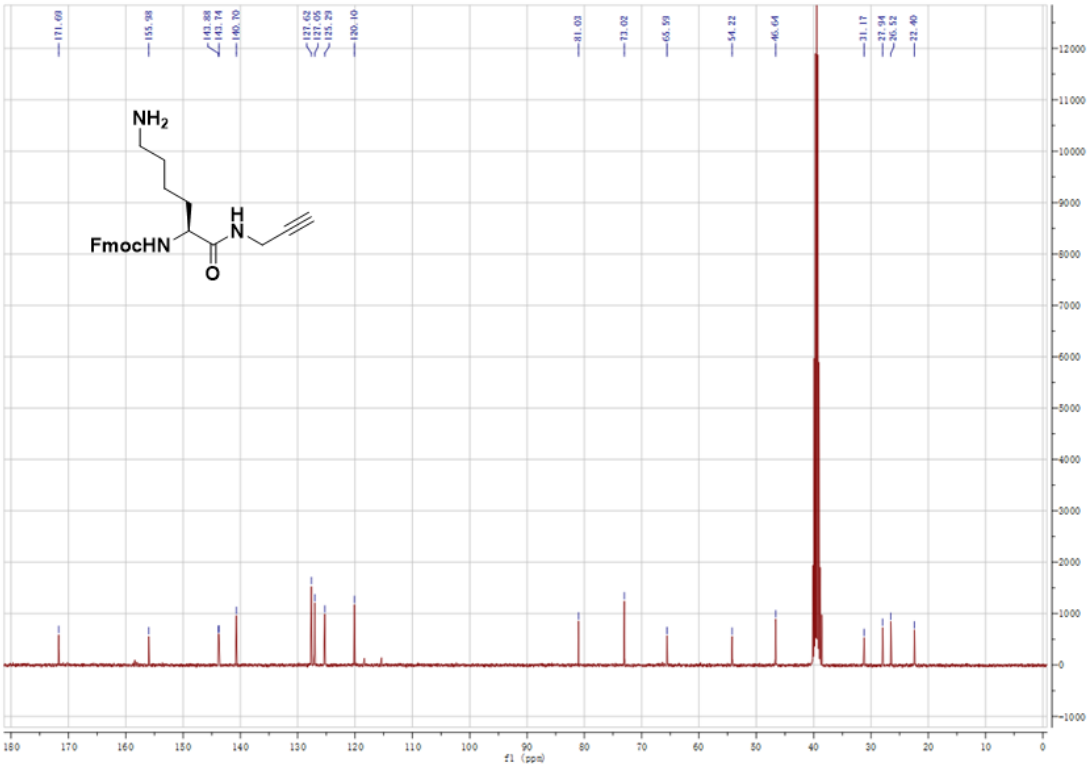

Figure S4. ^{13}C NMR spectrum of compound **2**.

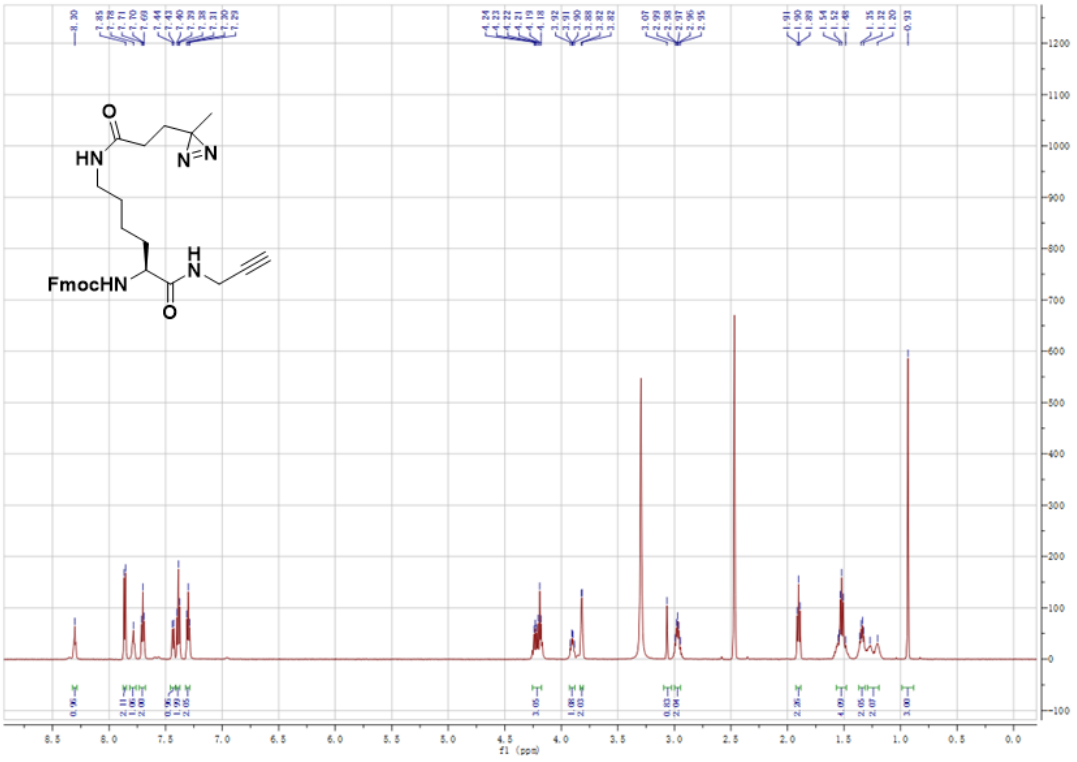

Figure S5. ^{1}H NMR spectrum of compound **3**.

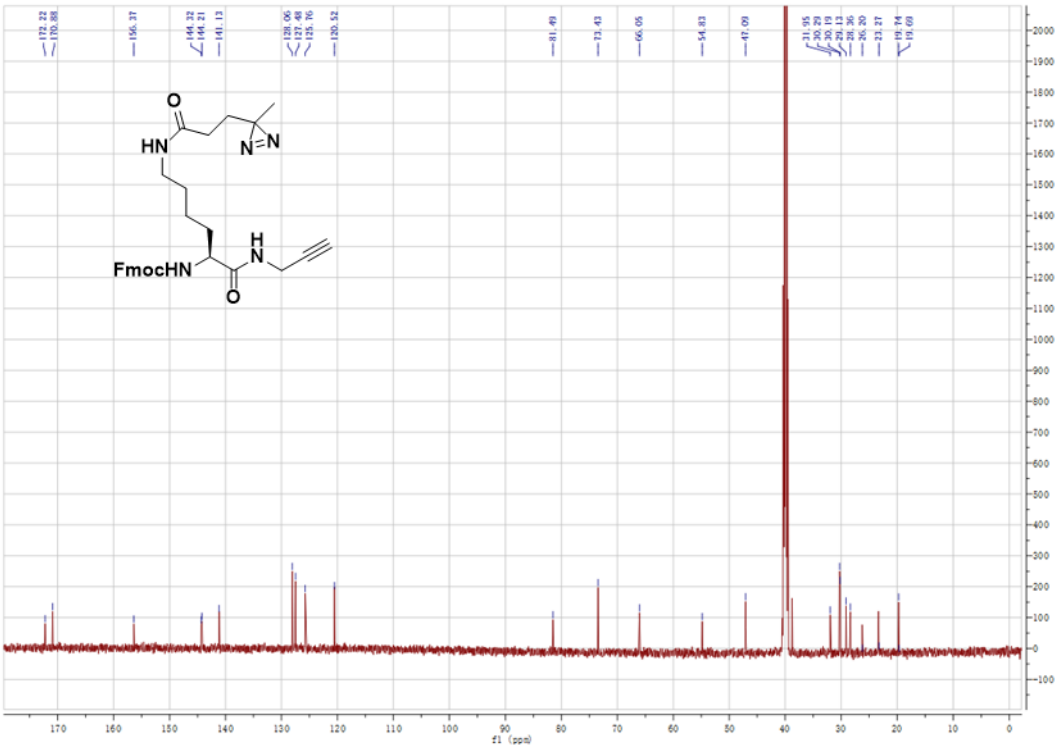

Figure S6. ^{13}C NMR spectrum of compound **3**.

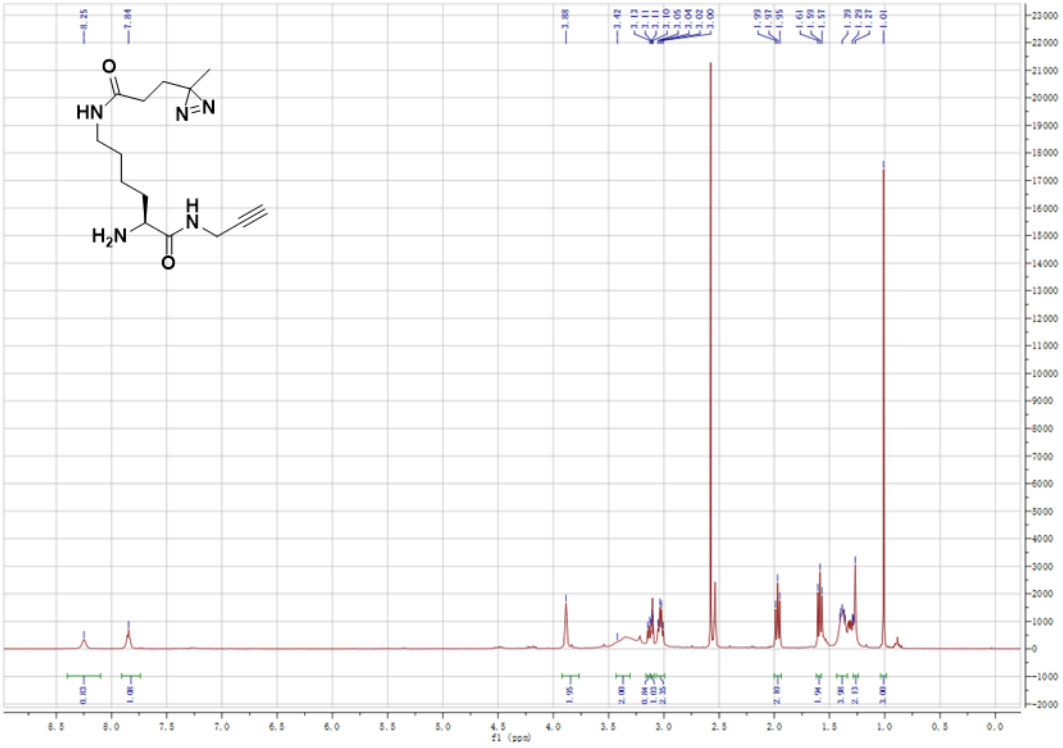

Figure S7. ^{1}H NMR spectrum of compound **4**.

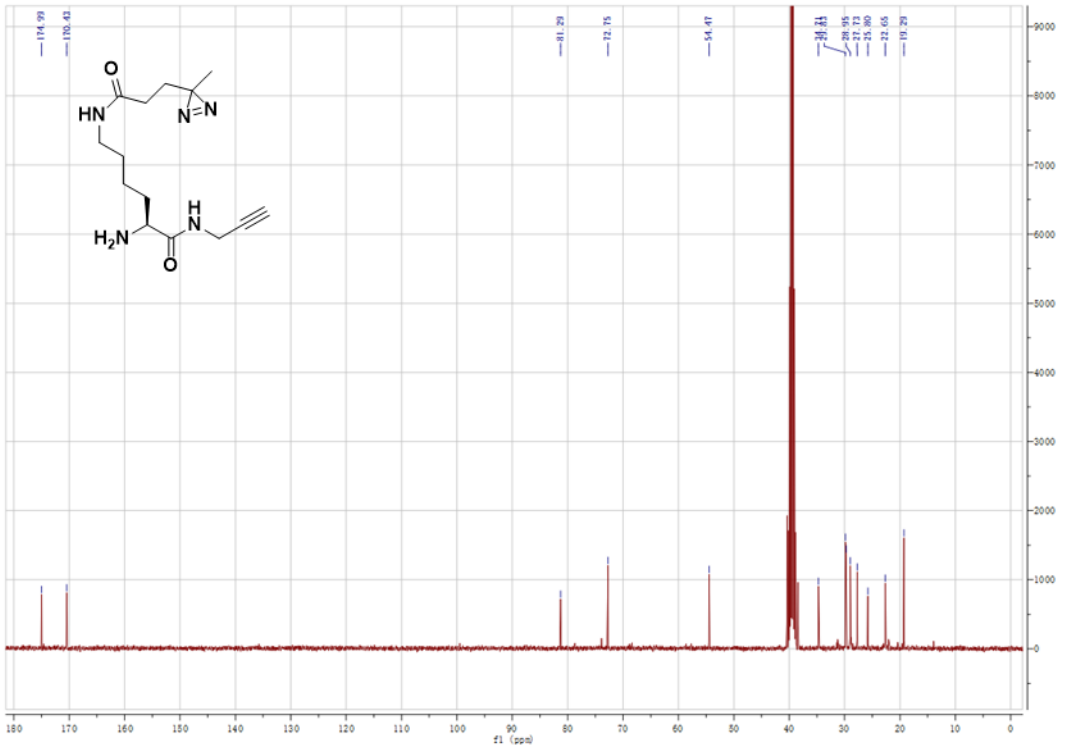

Figure S8. ^{13}C NMR spectrum of compound **4**.

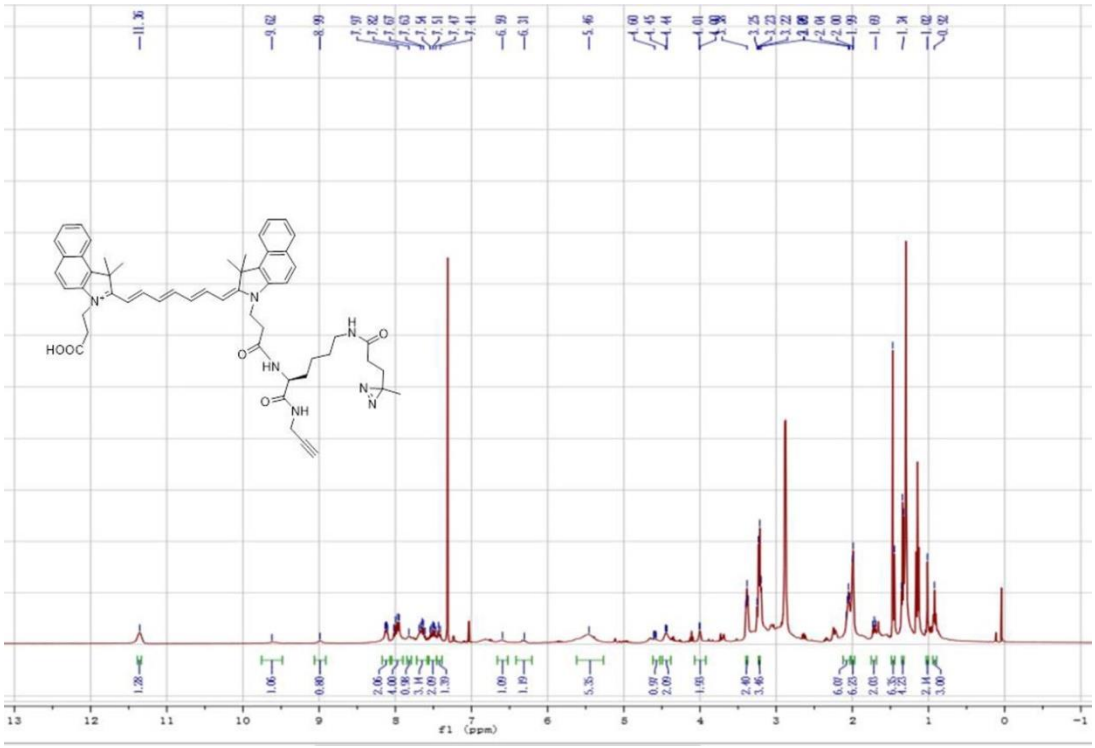

Figure S9. ^{1}H NMR spectrum of compound **5** in $CDCl_3$.

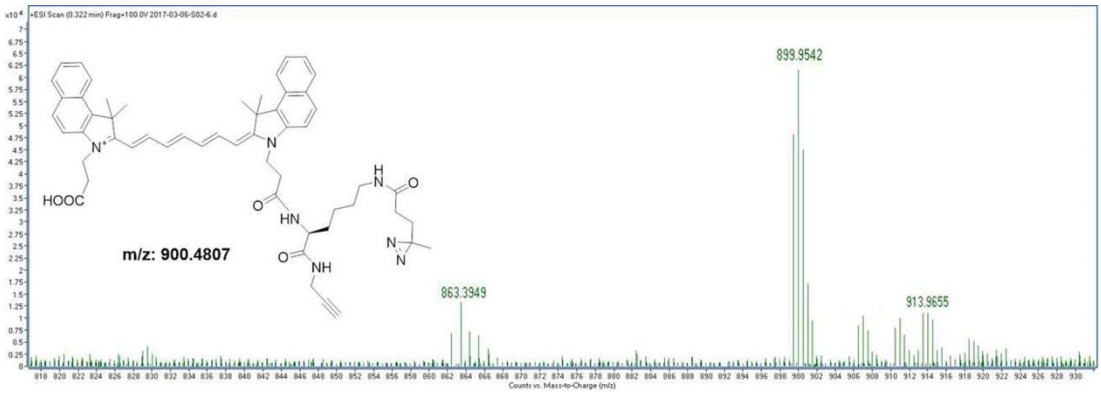

Figure S10. HR-MS spectrum of compound **5**.

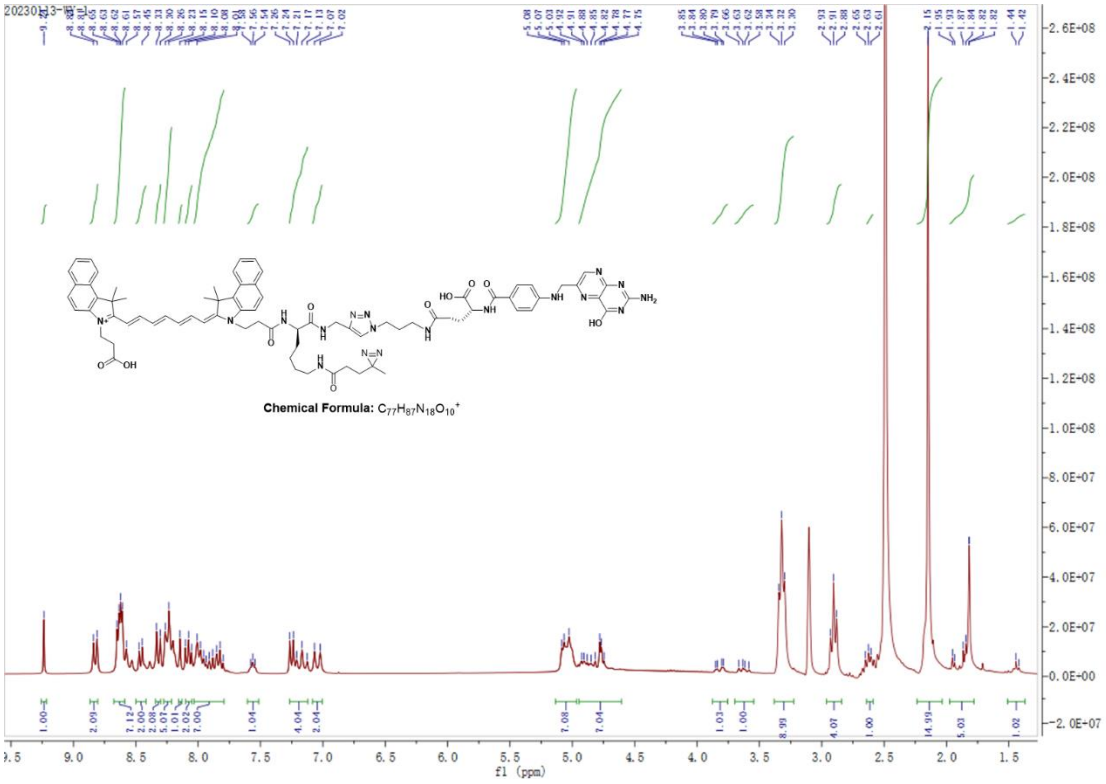

Figure S11. ^{1}H NMR spectrum of DACF.

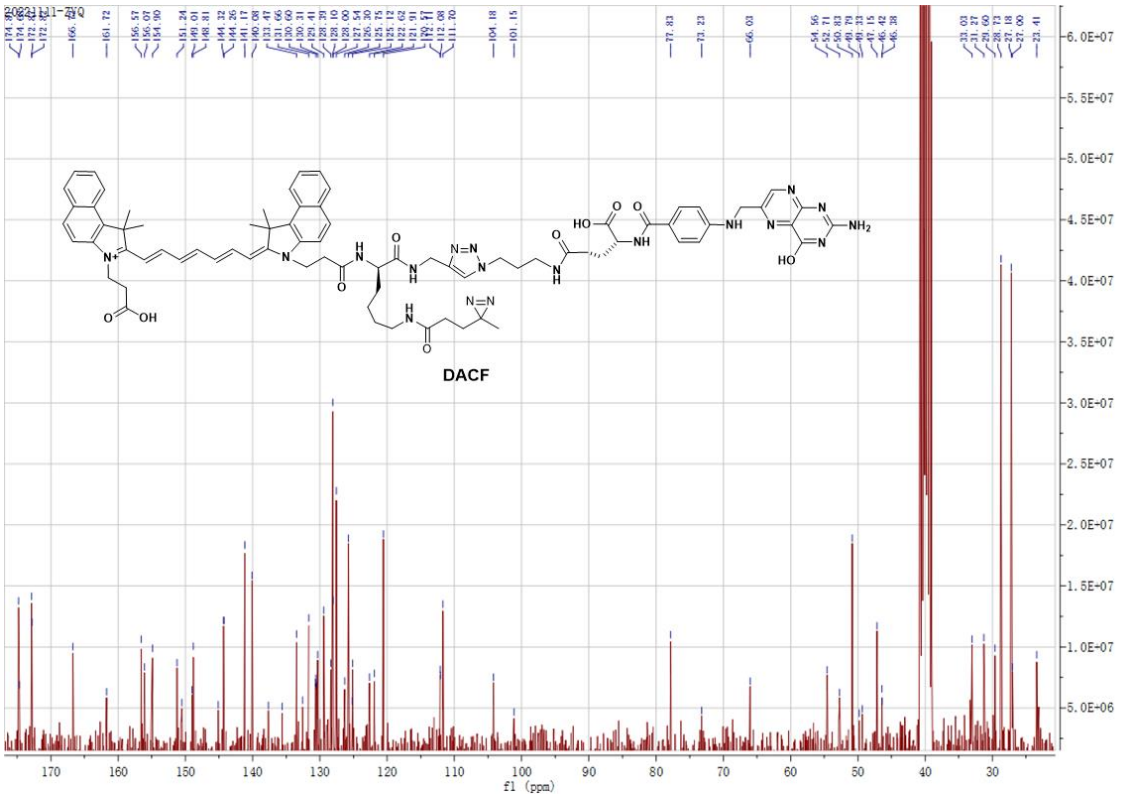

Figure S12. ^{13}C NMR spectrum of DACF

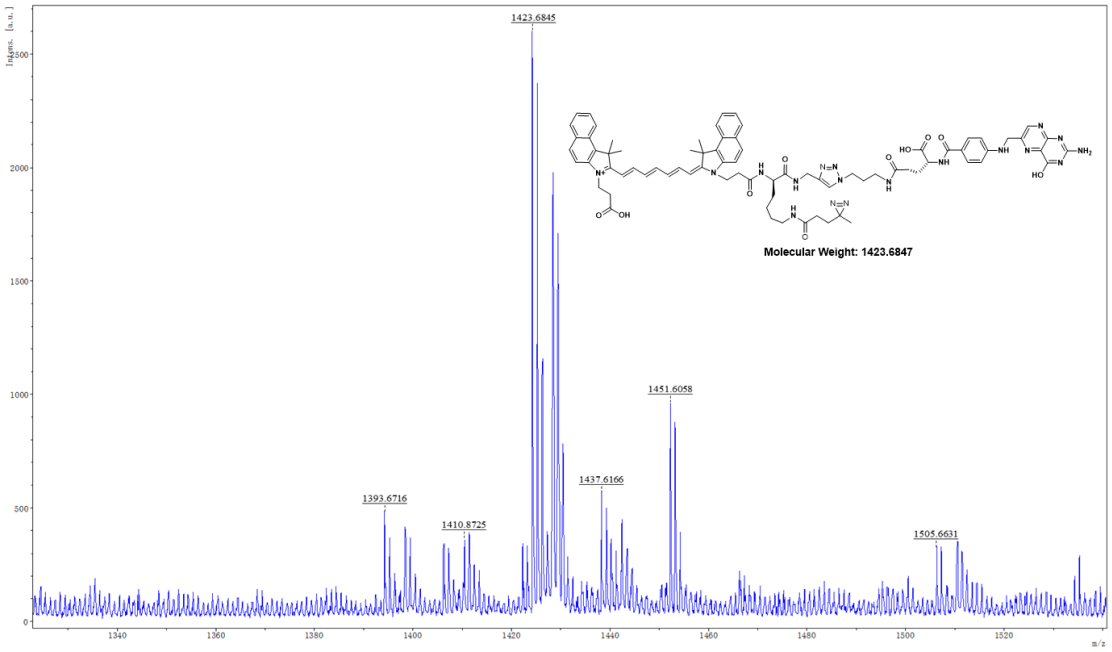

Figure S13. HR-MS spectrum of DACF.

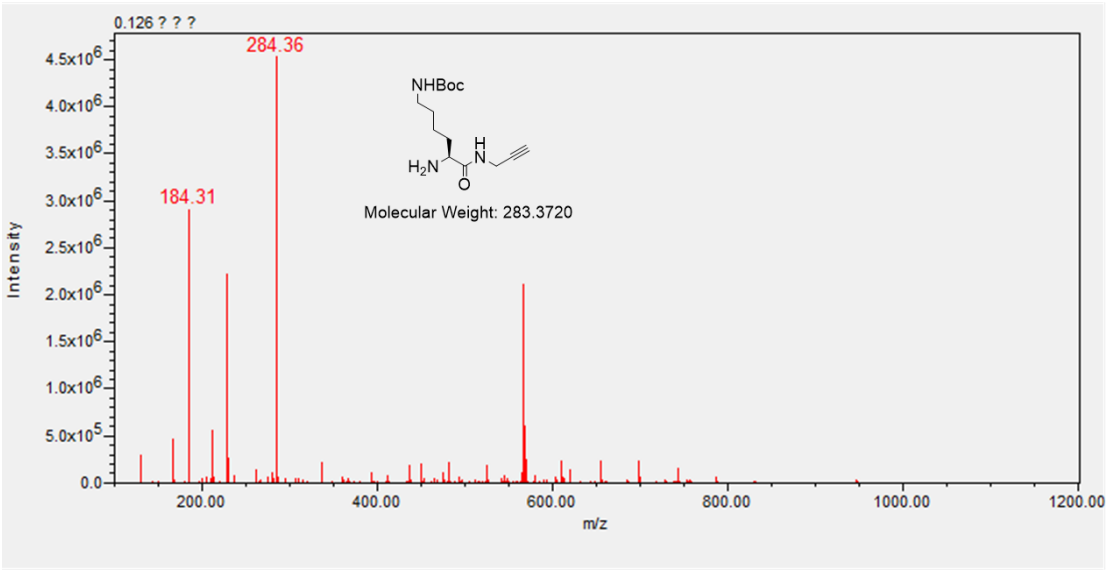

Figure S14. MS spectrum of compound **1'**.

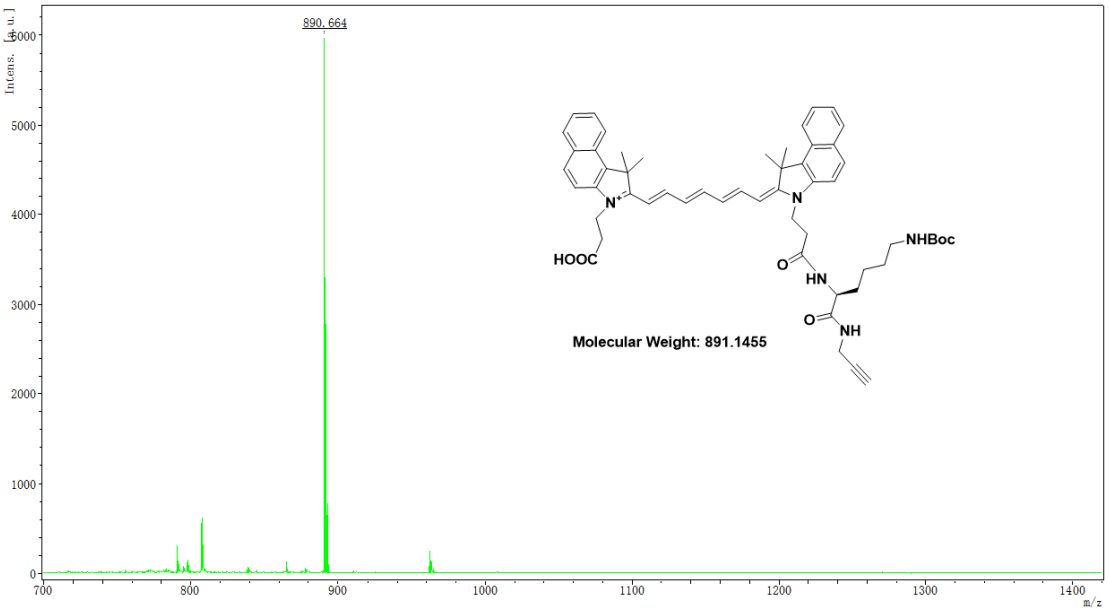

Figure S15. MS spectrum of compound **2'**.

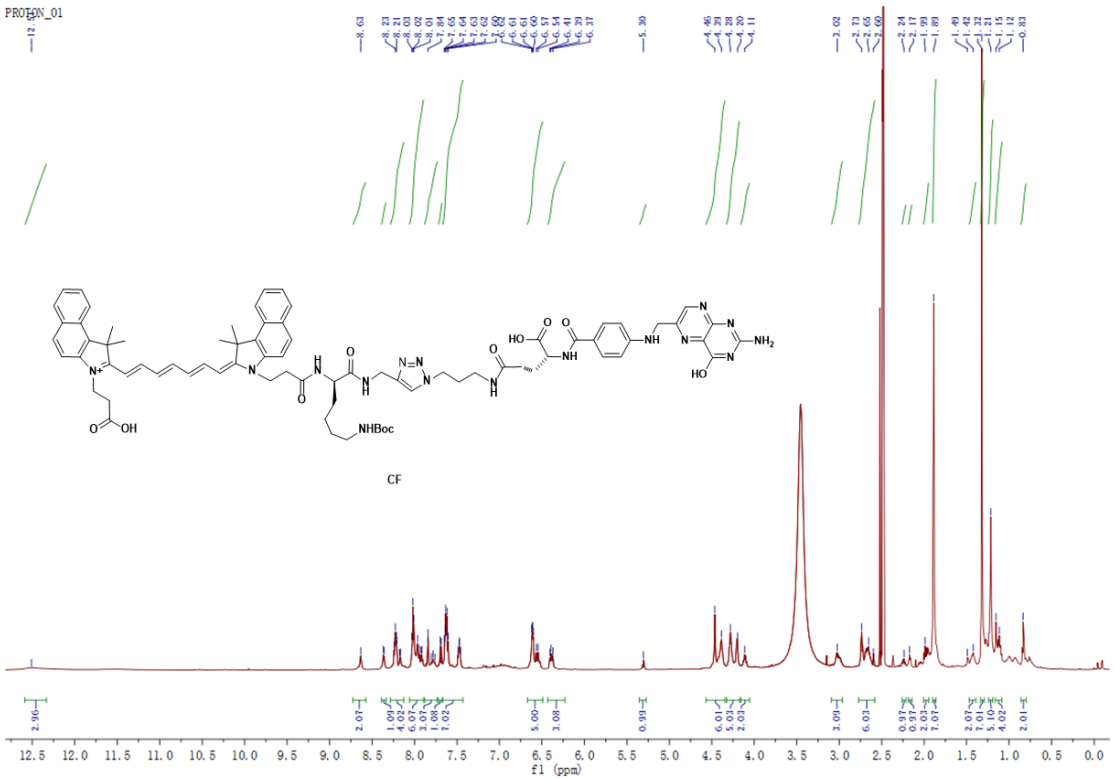

Figure S16. ^{1}H NMR spectrum of control probe CF.

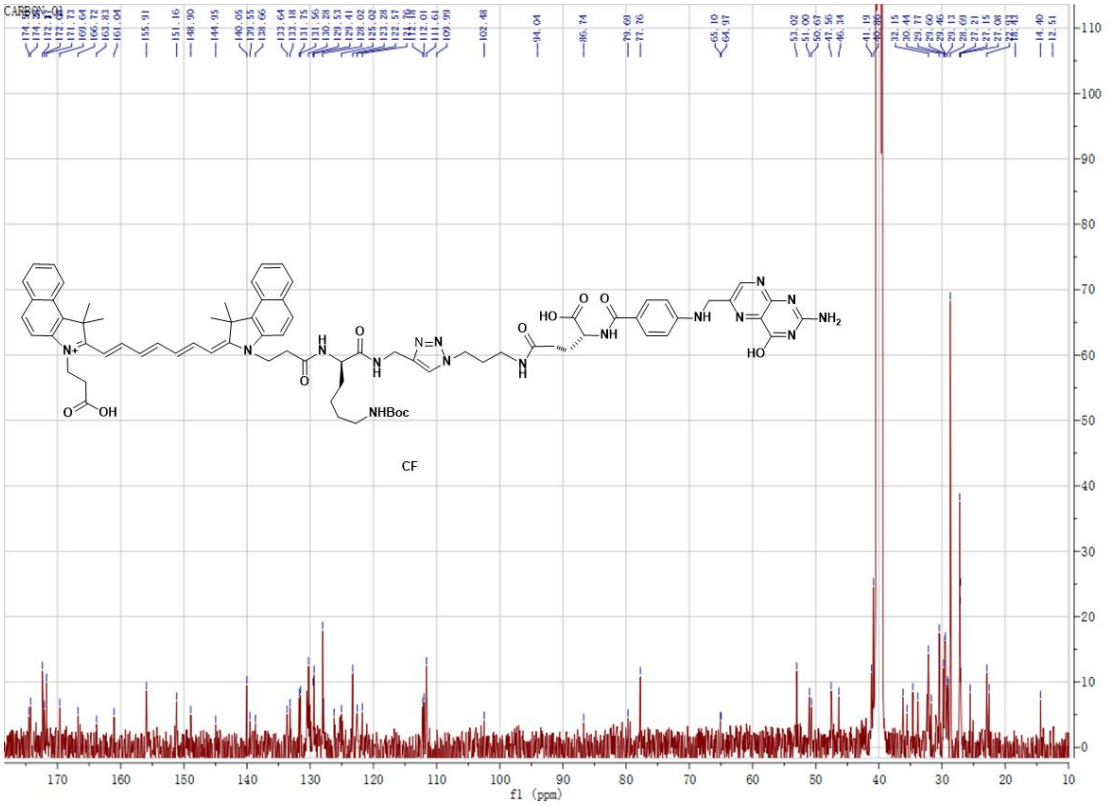

Figure S17. ^{13}C NMR spectrum of control probe CF.

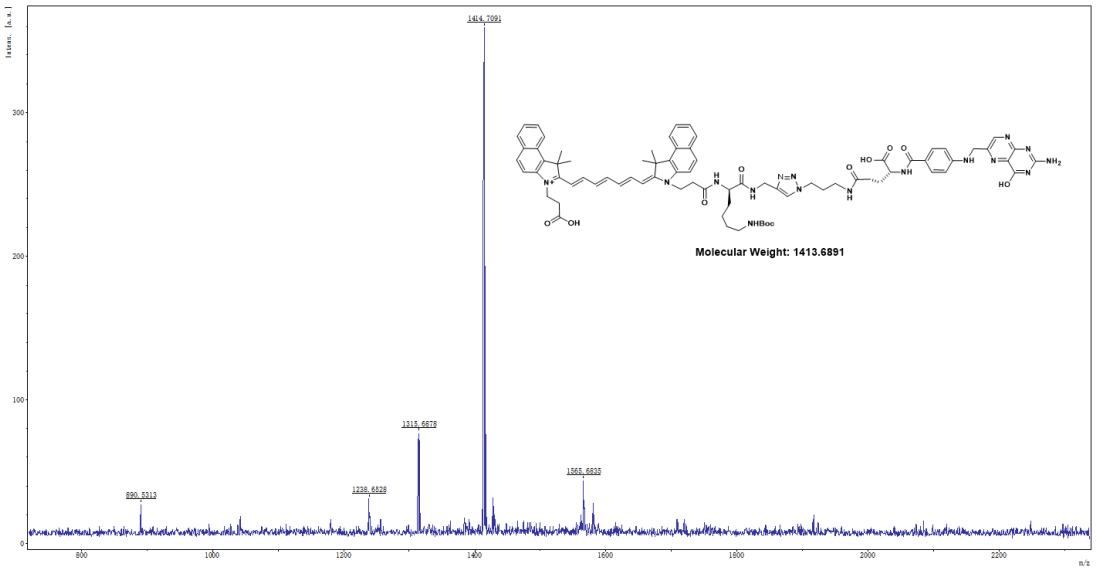

Figure S18. HR-MS spectrum of control probe CF.

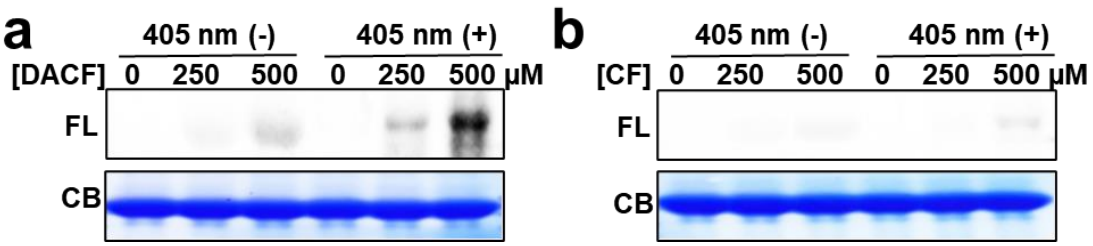

Figure S19. In-gel analysis of BSA labeling. SDS-PAGE of BSA (2.5 mg/mL) labeled by different concentrations of probe DACF (a) and CF (b) with or without 405 nm laser irradiation.

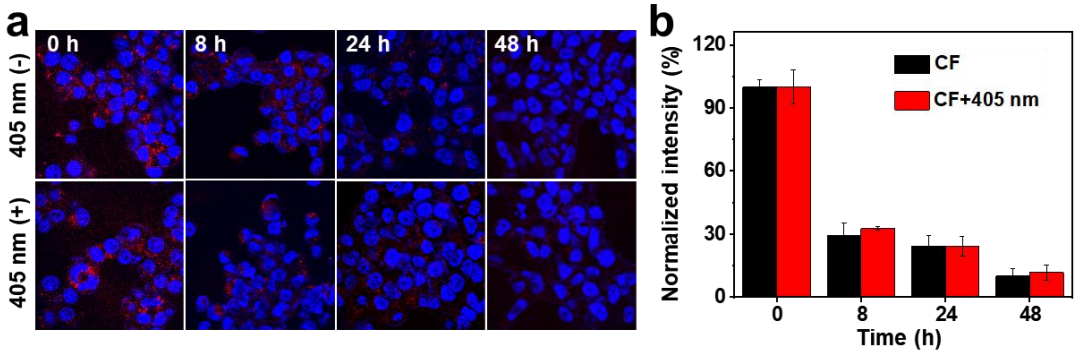

Figure S20. Cellular uptake of control probe CF. Real-time confocal imaging (a) and normalized intensity (b) of CF-treated 4T1 cells with (bottom) and without (top) 405 nm laser irradiation. Condition: 4T1 cells were incubated with CF (1 μM) for 12 h followed by 405 nm laser irradiation (1 W/cm^2, 1.5 min). λex/em = 635/(710 ± 50) nm. All images share the same scale bar (30 μm).

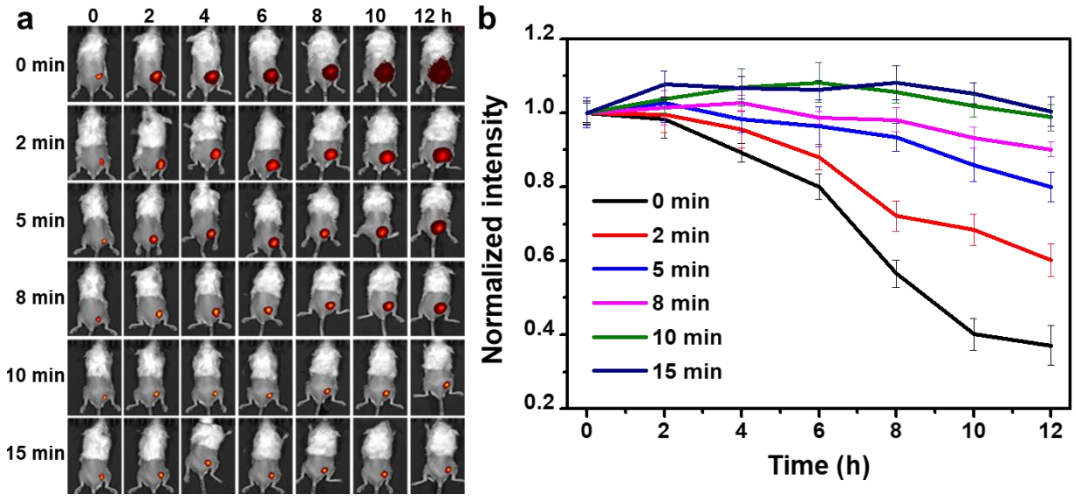

Figure S21. Time optimization of 405 nm irradiation for in vivo photoaffinity crosslinking. Six groups of BALB/c mice were subcutaneously administered with the same dosage of DACF (25 μL, 1 μM) at the right thigh and subsequently exposed to 405 nm laser irradiation (1 W/cm^2) for different times (0, 2, 5, 8, 10, and 15 min) followed by real-time fluorescence imaging using IVIS instrument. Fluorescence imaging (a) and normalized intensity (b) of mice were acquired at 0, 2, 4, 6, 8, 10, 12 h after irradiation.

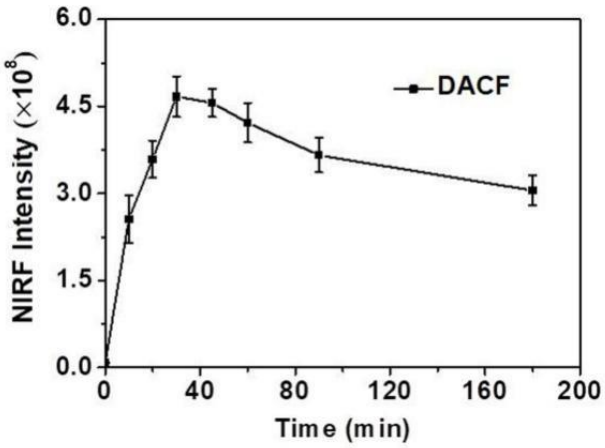

Figure S22. Real-time monitoring the accumulation of DACF in tumor region. Fluorescence intensities of the tumorous sites in mice intravenously injected with the DACF (45 μM, 200 μL) at different time (0, 10, 20, 30, 45, 60, 90, and 180 min).

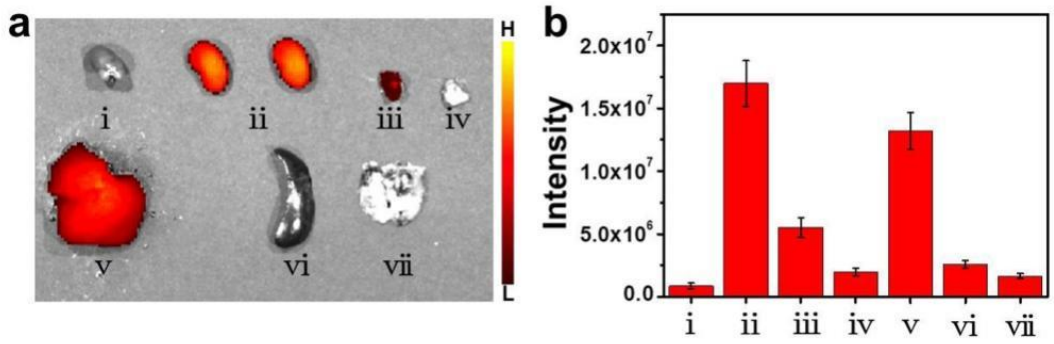

Figure S23. Biodistribution analysis of DACF in living mice. (a) ex vivo fluorescence images and (b) quantified fluorescent intensity of major organs and tumors dissected from the mice injected intravenously with the DACF (45 μM, 200 μL) after 24 h of 405 nm laser irradiation (i: heart, ii: kidney, iii: left tumor with 405 nm laser irradiation, iv: right tumor without 405 nm laser irradiation, v: liver, vi: spleen, vii: lung).

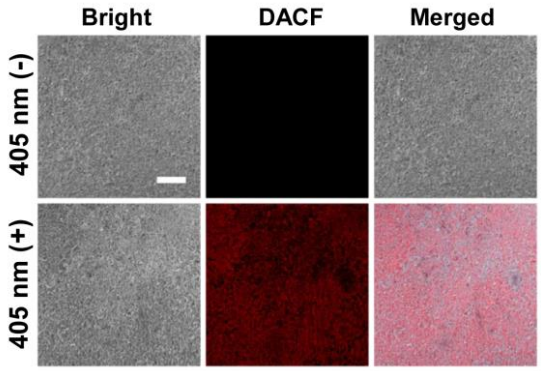

Figure S24. CLSM images of slices of tumor tissues dissected from the mice injected intravenously with the DACF (45 μM, 200 μL) after 24 h of 405 nm laser irradiation. All images share the same scale bar (120 μm).

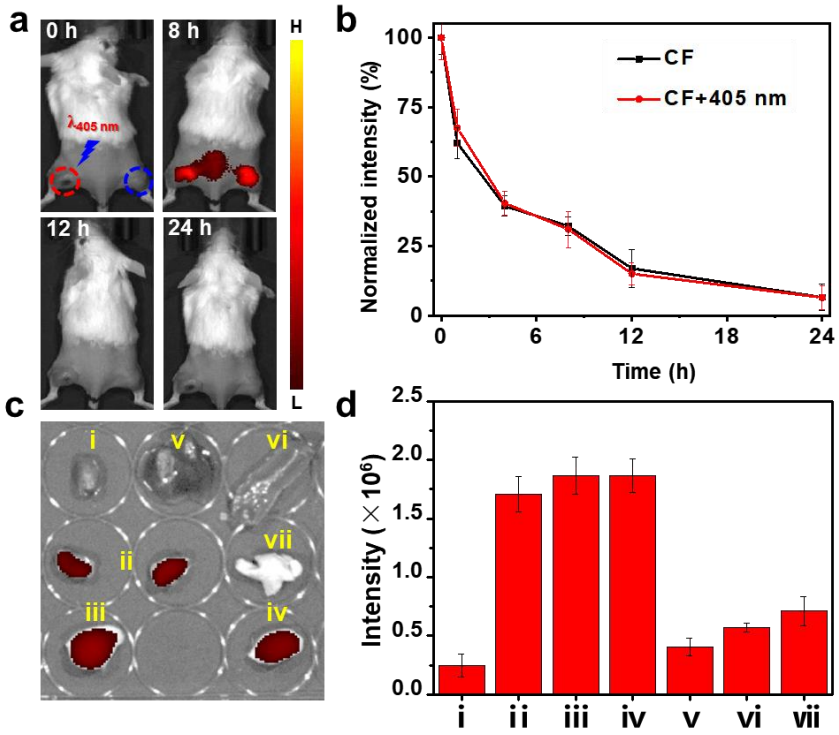

Figure S25. In vivo real-time tumor imaging. Fluorescence imaging (a) and normalized intensity (b) of 4T1 tumor-bearing mice with (tumor on the left) or without (tumor on the right) 405 nm laser irradiation 0.5 h posterior to intravenous injection of CF (45 μM, 200 μL). Images were acquired at 0, 8, 12, 24 h after 405 nm laser irradiation. Ex vivo fluorescence images (c) and quantified intensity (d) of major organs and tumors dissected from the mice at 24 h. 405 nm laser: 1 W/cm^2. λex/em = 745/(815 ± 25) nm (exposure time: 200 ms). Red circles point the tumor locations in mice, i: heart, ii: kidney, iii: left tumor with 405 nm laser irradiation, iv: right tumor without 405 nm laser irradiation, v: liver, vi: spleen, vii: lung).

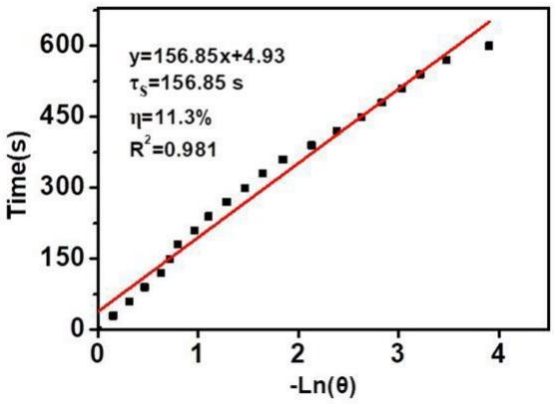

Figure S26. Linear time data versus−ln(θ) obtained from the cooling period and photothermal conversion efficiencies (η) of DACF.

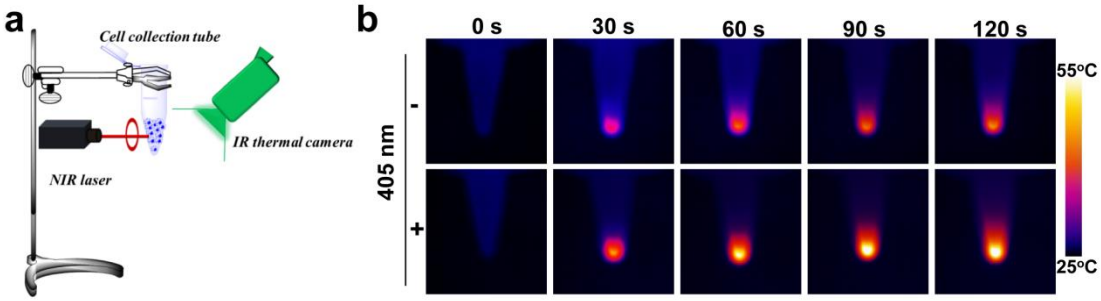

Figure S27. Characterization of photothermal effect. (a) Schematic diagram of 4T1 cells in a cell collection tube loaded with the DACF upon NIR irradiation. The red circle shows the area of laser illumination. The local temperature was monitored using an IR thermal camera. (b) Photothermal images of 4T1 cells loaded with the DACF against 808 nm laser irradiation after 48 h of 405 nm laser irradiation. 808 nm laser: 3 W/cm^2; 405 nm laser: 1 W/cm^2.

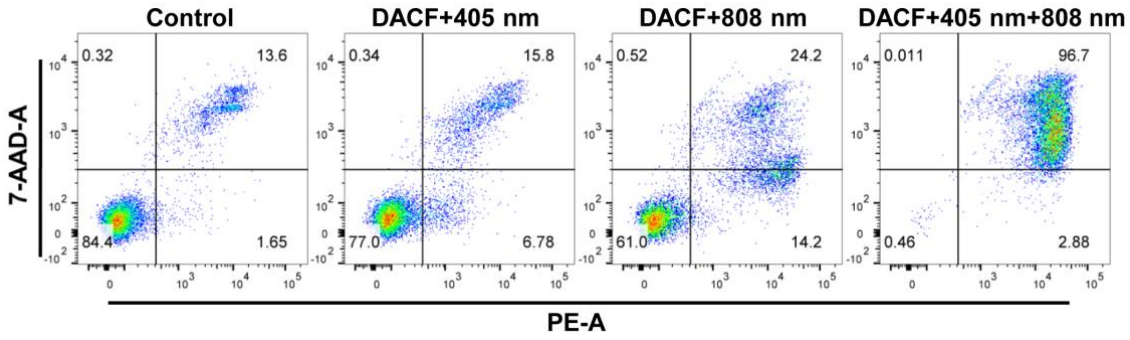

Figure S28. Apoptosis rates of 4T1 cells with various treatments (Control, DACF+405 nm, DACF+808 nm and DACF+405 nm+808 nm). 405 nm laser: 1 W/cm^2. 808 nm laser: 3 W/cm^2.

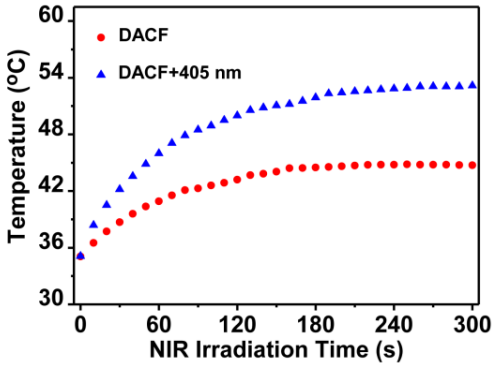

Figure S29. Hyperthermia heating curves of the tumors in mice intravenously injected with DACF (90 μM, 200 μL) with different treatments.

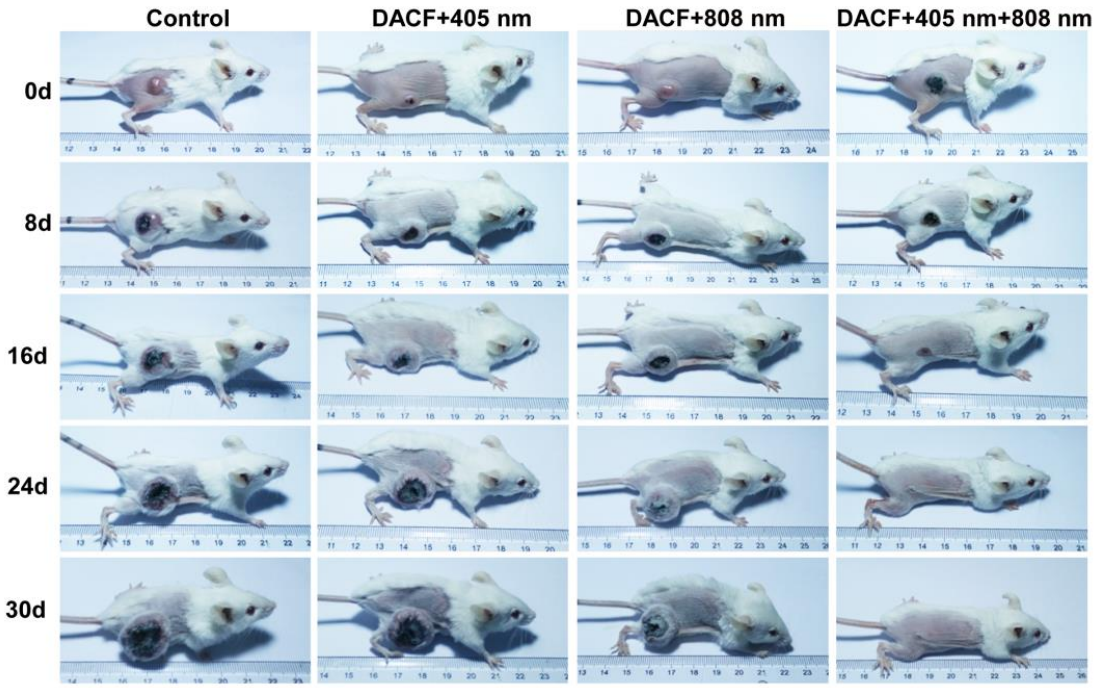

Figure S30. Representative tumor images of four group (Control, DACF+405 nm, DACF+808 nm and DACF+405 nm+808 nm) at 0, 8, 16, 24 and 30 day.

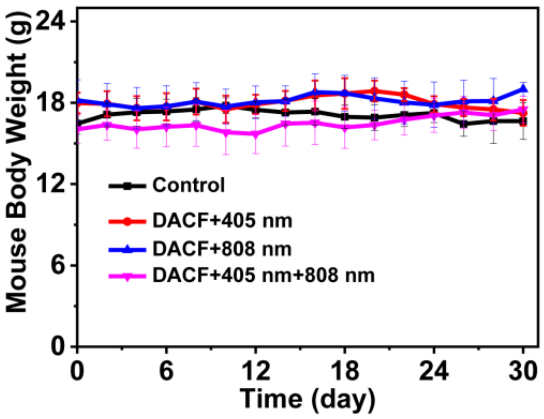

Figure S31. Average body weight of mice after various treatments (Control, DACF+405 nm, DACF+808 nm and DACF+405 nm+808 nm).

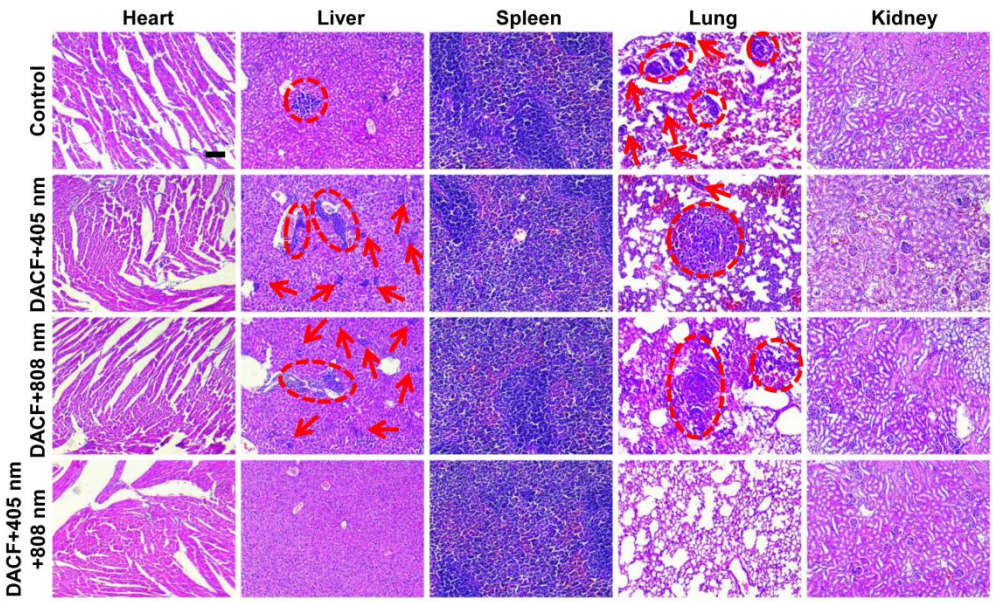

Figure S32. Micrographs of H&E stained heart, liver, spleen, lung and kidney slices collected from different groups of mice on 30th day. Tumor metastasis sites are highlighted by red circles and arrows. All images share the same scale bar (100 μm).

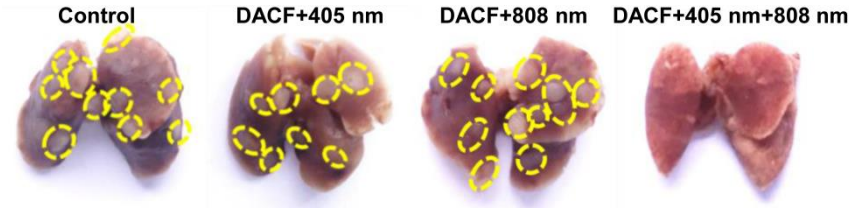

Figure S33. Images of a representative lung in mice from each group captured on 30th day after the treatment for showing the effects of different therapeutic combinations. Tumor metastasis sites are highlighted by yellow circles.

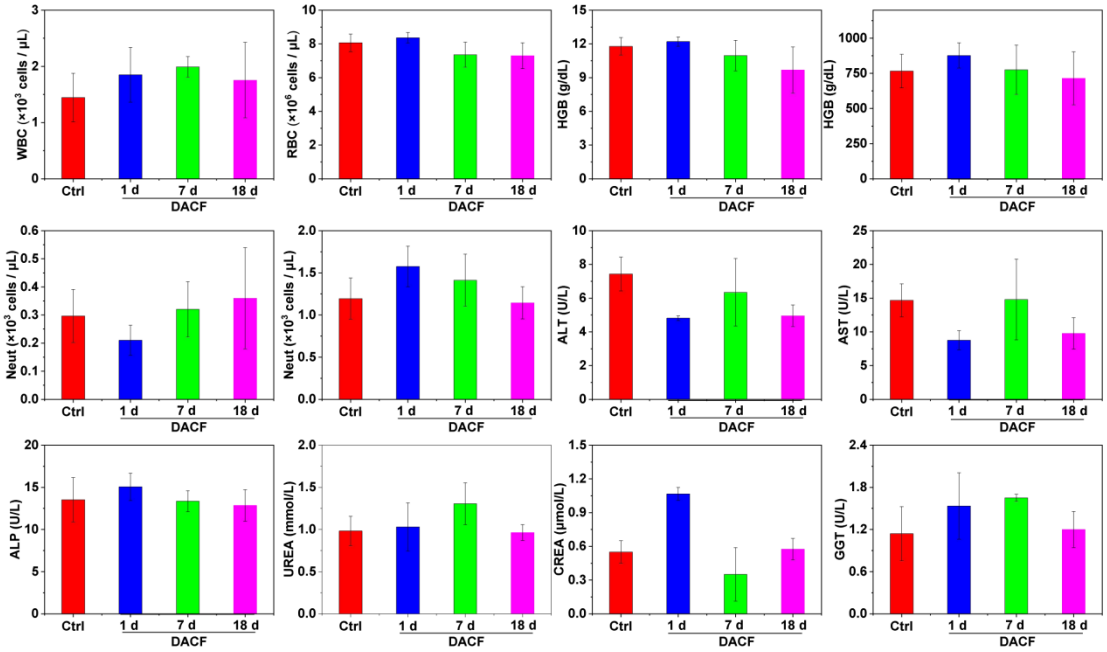

Figure S34. Blood routine and blood chemical analysis of mice receiving single intravenous injection of saline (control) or DACF after 1, 7, 18 days postinjection.

Reference

(1) Yin, L.; Sun, H.; Zhang, H.; He, L.; Qiu, L.; Lin, J. G.; Xia, H. W.; Zhang, Y. Q.; Ji, S-J.; Shi, H. B.; Gao, M. Y. Quantitatively Visualizing Tumor-Related Protease Activity in Vivo Using a Ratiometric Photoacoustic Probe. *J. Am. Chem. Soc*. **2019**, *141*, 3265−3273.